CHAPTER 3

3. Results and Discussion

3.1 Determination of Optimum Parameters

Flow injection analysis - mass spectrometry (FIA-MS) experiments were performed in order to determine the optimum heated nebuliser parameters for absolute sensitivity and signal to noise (S/N) ratio, as well as to select the appropriate ion for identification and quantification of the pesticides in the SIM LC-API-MS experiments.

3.1.1 Selection of Ionisation Mode[positive/negative chemical ionisation (PCI/NCI) for identification/quantification]

In preliminary experiments using full scan acquisitions containing 0.1 μg of the above mentioned standard pesticides, both positive and negative ionisation modes were evaluated. Table (10) shows the relative intensity (% of base peak) of the main fragment ions (m/z) in PCI and NCI modes at heated nebuliser probe temperature 300^{0}C, orifice 25 volts and focusing ring 30 volts.

	Mode of Ionisation	Fragment ions (m/z) Relative intensity		
Carbofuran	PCI	222.2(78.9)	165.3(100)	-
Carbaryl	PCI	202.4(14.7)	145.3(100)	-
Methiocarb	PCI	226.2(29.2)	169.3(100)	-
Diuron	PCI	233.1(100)	-	-
Chlorothalonil	NCI	245.0(100)	-	-
Ethyl-parathion	NCI	262.1(22.3)	138.1(100)	-
Endosulfan	NCI	405(22.1)	340.9(100)	-
Methamidophos	PCI	142.2(100)	125.2(30.2)	94.2(47.3)
	NCI	140.2(100)	126.1(12.0)	-
Dimethoate	PCI	230.2(100)	199.2(80.3)	171.3(26.7)
	NCI	214.1(100)	141.2(45.5)	-
Diazinon	PCI	305.3(100)	-	-
	NCI	275.0(44.5)	224.0(49.7)	169.2(100)
chlorpyrifos	PCI	350.1(100)	198.1(25.2)	-
	NCI	329.9(100)	169.2(51.6)	-
Profenofos	PCI	375.0(100)	347.1(41.7)	304.9(16.7)
	NCI	344.9(20.4)	284.8(10.7)	205.0(100)
Malathion	PCI	331.2(52.6)	285.1(100)	127.1(73.7)
	NCI	314.7(24.0)	157.0(100)	

Table (10) - The relative intensity (% of base peak) of the main fragment ions in FIA-API-MS of the pesticides in PCI and NCI modes at heated nebuliser temperature 300^{0}C, orifice 25 volts and focusing ring 30 volts.

The pesticides can be classified into 3 groups:- Group 1- those which are detectable by only PCI mode, Group 2 - those which are detectable by only NCI mode and Group 3- detectable by both PCI/NCI modes. Table (11) shows the classification of pesticides by detectable ionisation mode.

Group 1 (PCI mode only)	Group 2 (NCI mode only)	Group 3 (PCI/NCI mode)
Carbofuran	Chlorothalonil	Methamidophos
Carbaryl	Ethyl-Parathion	Dimethoate
Methiocarb	Endosulfan	Diazinon
Diuron		Chlorpyrifos
		Profenofos
		Malathion

Table 11 -Classification of pesticides by detectable Ionisation mode in FIA-API-MS

Before optimisation, the mass spectrum of each compound was recorded in order to select the most abundant mass-to-charge ratio (m/z) for further studies. For all the compounds in Group1, the protonated $(M+H)^+$ pseudo-molecular ion were registered. Diuron is a phenylurea herbicide. Fig. (11) shows the mass spectrum of diuron under PCI mode, the $[M+H]^+$ pseudo-molecular ion of high intensity was registered as the base peak. Fig. (12) shows the proposed fragmentation scheme of diuron under PCI mode.

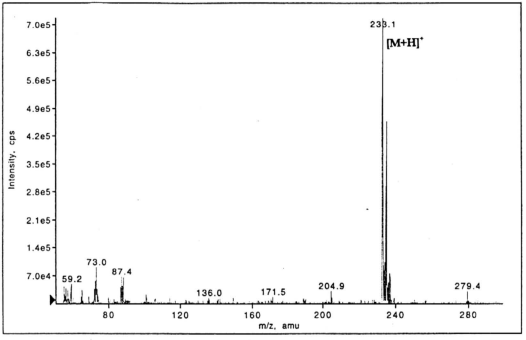

Fig.(11) -The mass spectrum of diuron under PCI mode. The protonated $[M+H]^+$ pseudo-molecular ion registered as base peak

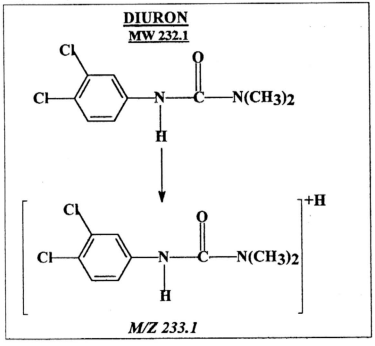

Fig. (12) - The proposed fragmentation scheme of diuron under PCI mode.

Fig.(13) shows the mass spectrum of diuron under NCI mode in which no ion attributable to diuron was observed.

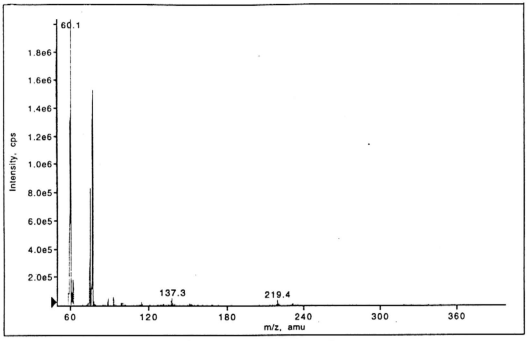

Fig. (13) - The mass spectrum of Diuron under NCI mode in which no fragment ion attributable to diuron was observed.

Whereas for NMC pesticides; carbofuran, carbaryl and methiocarb show specific fragmentation process under PCI condition, the loss of methylisocyanate (CH_3NCO) from the protonated pseudo-molecular ion gives rise to the exhibited base peaks of $[M+H-CONCH_3]^+$ or $[M-56]^+$ fragment ion in their respective mass spectrum (156). This phenomenon provides some structural confirmation for NMCs and are very likely due to thermal degradation of these compounds. Fig.(14,15,16) show the mass spectra of carbofuran, carbaryl and methiocarb. The proposed fragmentation schemes of the above mentioned compounds are as shown in Fig. (17,18, 19)

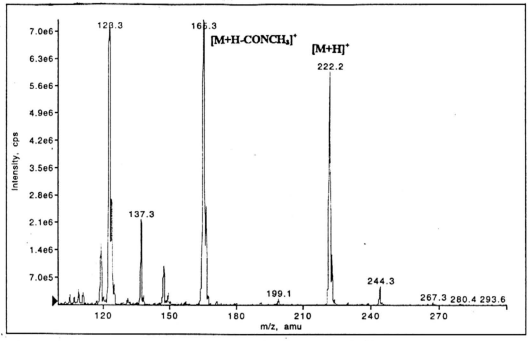

Fig.(14) -The mass spectrum of carbofuran under PCI mode. The protonated $[M+H]^+$ pseudo-molecular ion losses a methylisocyanate $[CH_3NCO]$ to exhibit a base peak at $[M+H-CH_3NCO]^+$ fragment ion or m/z 165.3. (156)

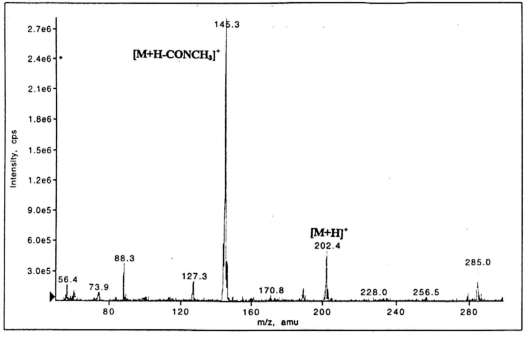

Fig. (15) - The mass spectrum of carbaryl under PCI mode. The protonated $[M+H]^+$pseudo-molecular ion losses a methylisocyanate $[CH_3NCO]$ to exhibit a base peak at $[M+H-CH_3NCO]^+$ fragment ion or m/z 145.3 (156)

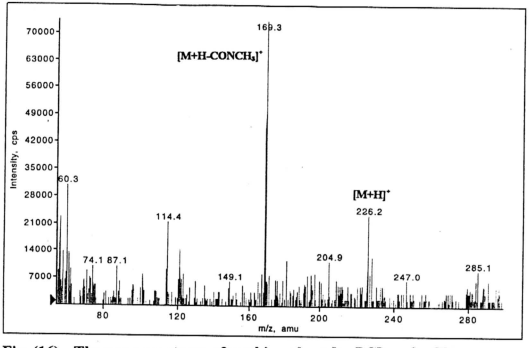

Fig. (16) - The mass spectrum of methiocarb under PCI mode. The protonated $[M+H]^+$ pseudo-molecular ion losses a methylisocyanate $[CH_3NCO]$ to exhibit a base peak at $[M+H-CH_3NCO]^+$ fragment ion or m/z 169.3 (156)

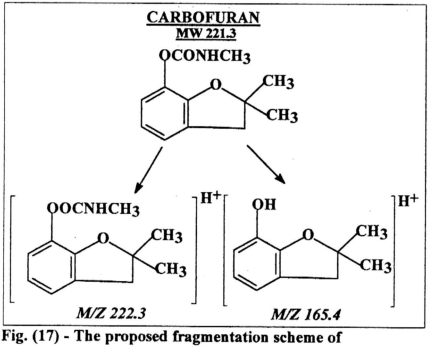

Fig. (17) - The proposed fragmentation scheme of carbofuran under PCI mode.

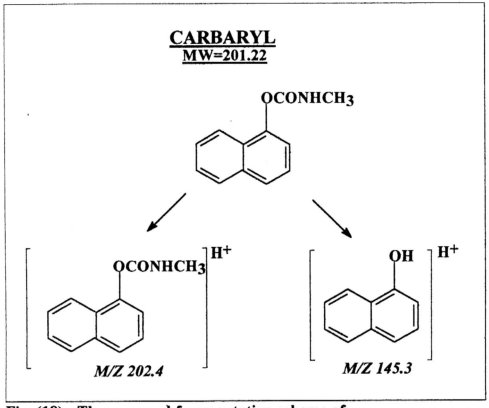

Fig. (18) - The proposed fragmentation scheme of carbaryl under PCI mode.

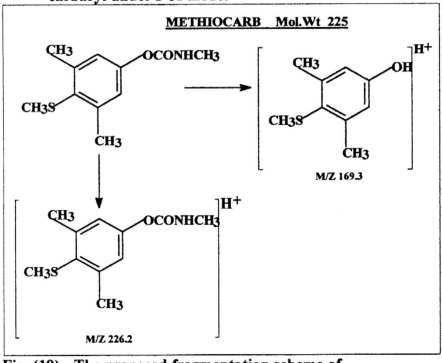

Fig. (19) - The proposed fragmentation scheme of methiocarb under PCI mode.

The low intensity of the pseudo-molecular ion $[M+H]^+$ in the mass spectra of the above mentioned NMCs made it essential to use the $[M+H-CONCH_3]^+$ fragment ion monitoring for quantitative analysis. For diuron, the high intensity of the protonated $[M+H]^+$ pseudo-molecular ion made it the only ion available to be monitored under SIM mode for identification and quantification purposes.

The pesticides in Group 2 respond only in NCI mode, Fig (20) show the mass spectrum of chlorothalonil under NCI mode. Chlorothalonil is a interhalogen compound, the ion minus a chlorine atom is first obtained from the molecule and then replaced by an oxygen atom to produce a distinct base peak at $(M-Cl+O)^-$ or (M-19) (163). Fig. (21) shows the proposed fragmentation scheme of chlorothalonil under NCI mode.

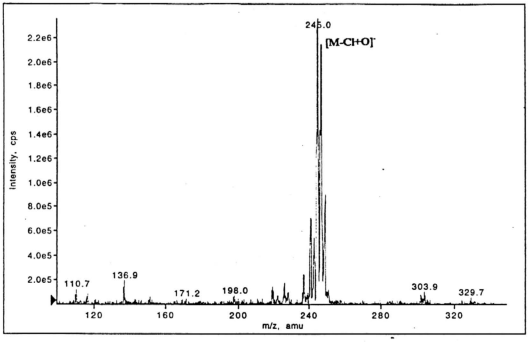

Fig.(20) -The mass spectrum of chlorothalonil under NCI mode. The $[M-Cl+O]^-$ or $[M-19]^-$ fragment ion exhibit as base peak. (163)

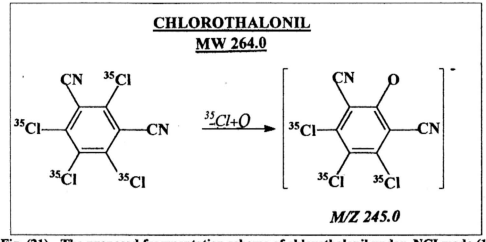

Fig. (21) - The proposed fragmentation scheme of chlorothalonil under NCI mode (163).

The high intensity of this ion makes it possible to achieve high specificity and therefore highly specific analysis can be performed by monitoring this ion for quantitative purposes. Fig.(22) shows the mass spectrum of chlorothalonil under PCI mode in which no ion attributable to chlorothalonil was observed.

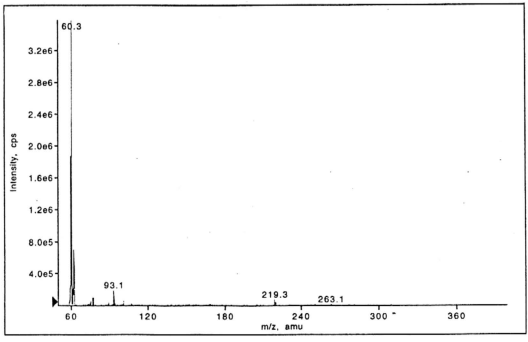

Fig.(22) -The mass spectrum of chlorothalonil under PCI mode.

Ethyl-parathion shows a demonoalkylation process which exhibits the fragment ion $[M\text{-}C_2H_5]^-$ followed by a replacement with an ether bond in the NCI mode (163). Fig. (23, 24) shows the mass spectrum and the proposed fragmentation scheme of ethyl-parathion under NCI mode respectively.

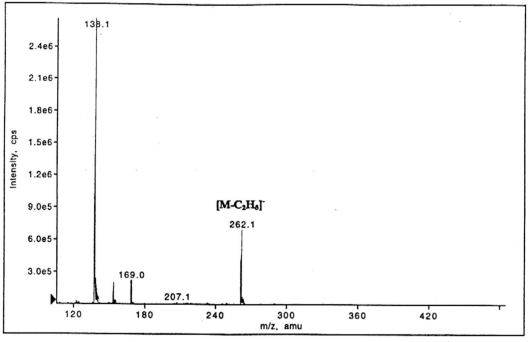

Fig. (23) - The mass spectrum of ethyl-parathion under NCI mode exhibits a distinct peak at m/z 262.1 $[M\text{-}C_2H_5]^-$ or $[M\text{-}29]^-$ fragment ion (163).

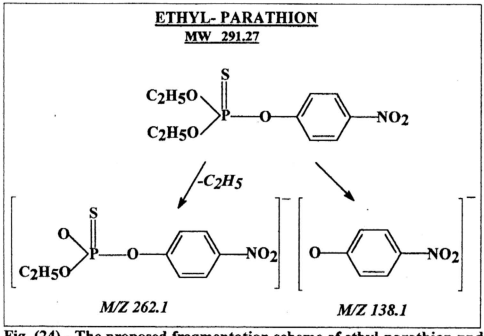

Fig. (24) - The proposed fragmentation scheme of ethyl-parathion under NCI mode.

When ethyl-parathion was analysed under PCI mode, the mass spectrum in Fig (25) showed no ion which can be attributed to the compound.

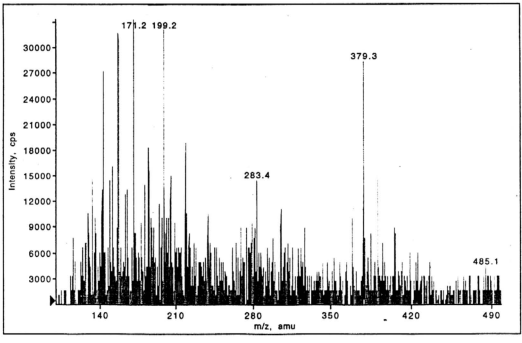

Fig. (25) - The mass spectrum of ethyl-parathion under PCI mode.

Endosulfan (purity 99.6% , purchased from AccuStandard Inc., New Haven CT, USA.) undergoes a deprotonation process to exhibit a $[M-H]^-$ pseudo-molecular ion peak which can be used for identification and quantification purposes. Fig. (26) shows the mass spectrum of endosulfan under NCI mode.

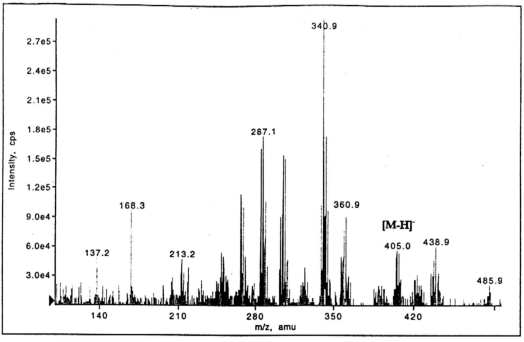

Fig.(26) -The mass spectrum of endosulfan (MW 406) under NCI mode.

In Group 3, all the 6 pesticides exhibit the protonated $[M+H]^+$ pseudo-molecular ion of high intensity under PCI mode, Fig. (27-32) show the mass spectra of methamidophos, dimethoate, diazinon, chlorpyrifos, profenofos and malathion under PCI mode respectively. Fig. (33-38) show the proposed fragmentation schemes of methamidophos, dimethoate, diazinon, chlorpyrifos, profenofos and malathion respectively.

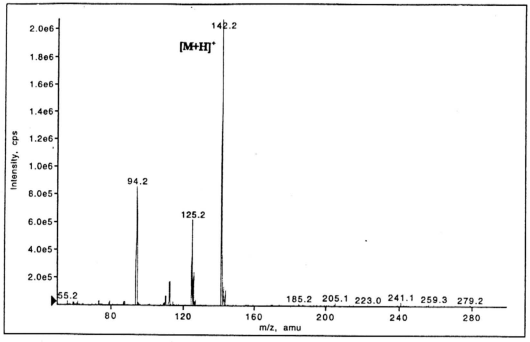

Fig.(27) -The mass spectrum of methamidophos exhibits a base peak at m/z 142.2 $[M+H]^+$ protonated pseudo-molecular ion under PCI mode.

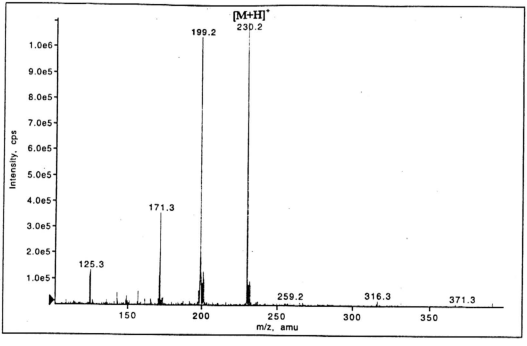

Fig.(28) -The mass spectrum of dimethoate shows a base peak at m/z 230.2 $[M+H]^+$ protonated pseudo-molecular ion under PCI mode.

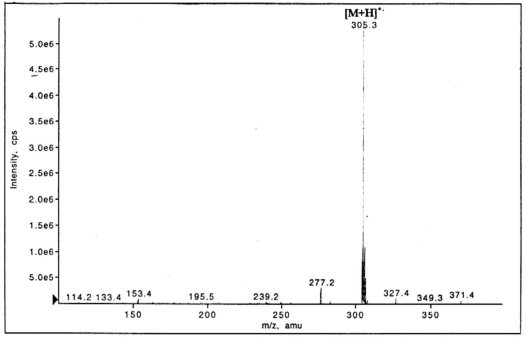

Fig.(29) -The mass spectrum of diazinon exhibits a base peak at m/z 305.3 $[M+H]^+$ protonated pseudo-molecular ion under PCI mode.

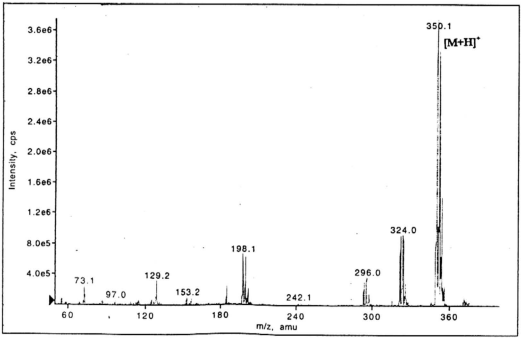

Fig.(30) -The mass spectrum of chlorpyrifos exhibits a base peak at m/z 350.1 $[M+H]^+$ protonated pseudo-molecular ion under PCI mode.

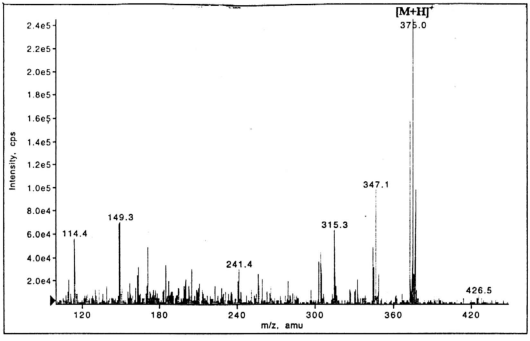

Fig. (31) - The mass spectrum of profenofos exhibits a base peak at m/z 375.0 $[M+H]^+$ protonated pseudo-molecular ion under PCI mode.

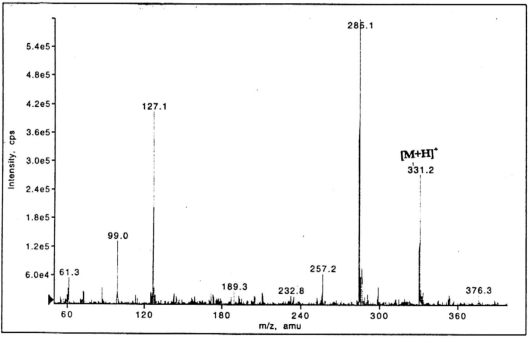

Fig. (32) - The mass spectrum of malathion exhibits a distinct peak at m/z 331.2 $[M+H]^+$ protonated pseudo-molecular ion under PCI mode.

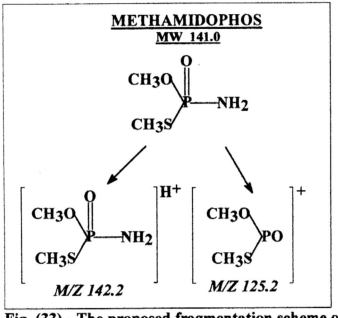

Fig. (33) - The proposed fragmentation scheme of methamidophos under PCI mode.

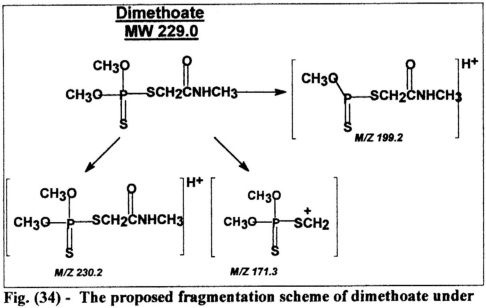

Fig. (34) - The proposed fragmentation scheme of dimethoate under PCI mode.

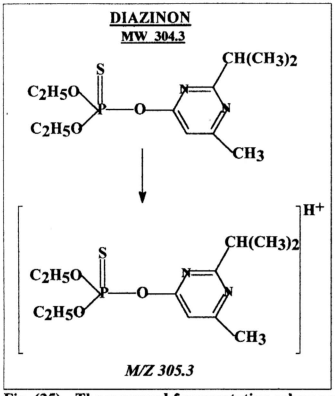

Fig. (35) - The proposed fragmentation scheme of diazinon under PCI mode.

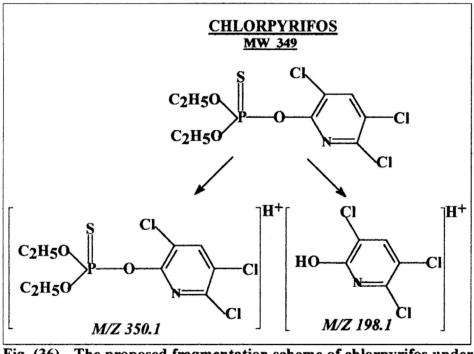

Fig. (36) - The proposed fragmentation scheme of chlorpyrifos under PCI mode

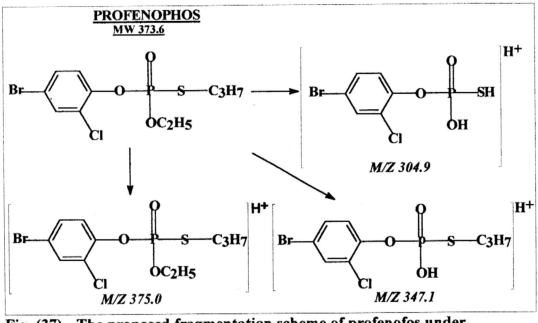

Fig. (37) - The proposed fragmentation scheme of profenofos under PCI mode.

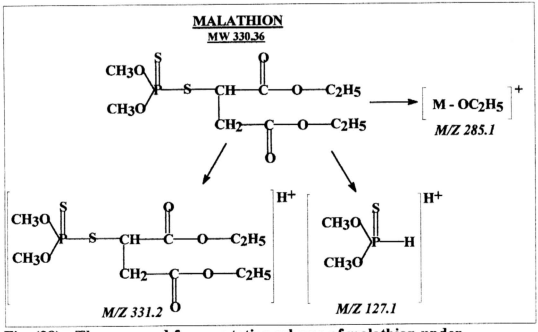

Fig. (38) - The proposed fragmentation scheme of malathion under PCI mode.

In NCI mode, methamidophos produces a deprotonated pseudo-molecular ion $[M-H]^-$ as the base peak. Fig. (39,40) shows the mass spectrum and its proposed fragmentation scheme respectively.

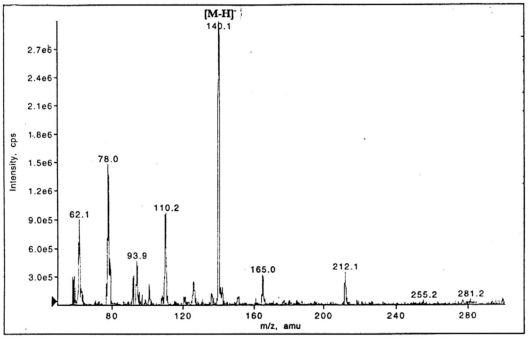

Fig.(39) -The mass spectrum of methamidophos exhibits a base peak at m/z 140.2 $[M-H]^-$ deprotonated pseudo-molecular ion under NCI mode.

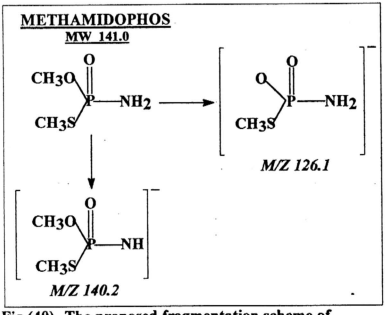

Fig.(40) -The proposed fragmentation scheme of methamidophos under NCI mode.

Dimethoate, diazinon, profenofos and malathion undergo demonoalkylation process to produce the $[M - R]^-$ ion where R = alkyl group(163). Fig (41-44) show the mass spectra of dimethoate, diazinon, profenofos and malathion under NCI mode respectively . Fig. (45-48) show the proposed fragmentation schemes of dimethoate, diazinon, profenofos and malathion respectively.

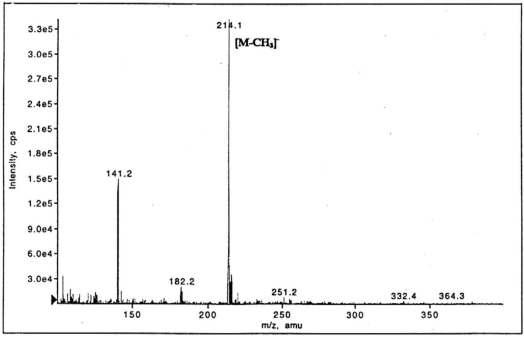

Fig.(41) -The mass spectrum of dimethoate exhibits a base peak at m/z 214.1 $[M-CH_3]^-$ or $[M-15]^-$ fragment ion under NCI mode.

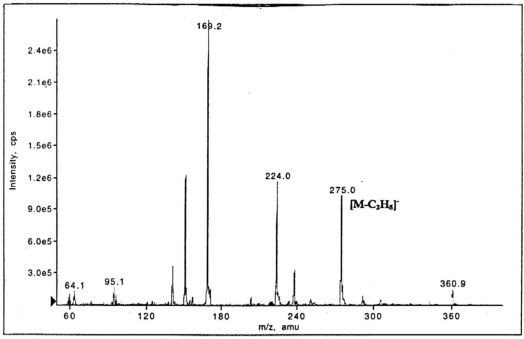

Fig.(42) -The mass spectrum of diazinon exhibits a distinct peak at m/z 275.0 $[M-C_2H_5]^-$ or $[M-29]^-$ fragment ion under NCI mode(163).

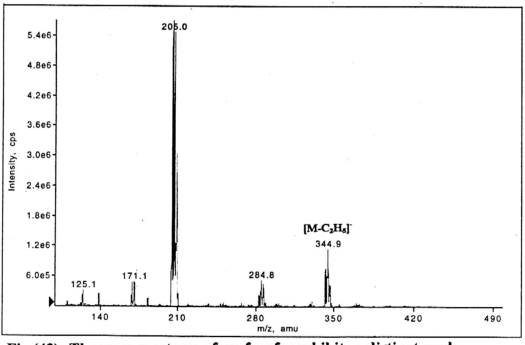

Fig.(43) -The mass spectrum of profenofos exhibits a distinct peak at m/z 344.9 $[M-C_2H_5]^-$ or $[M-29]^-$ fragment ion under NCI mode(163).

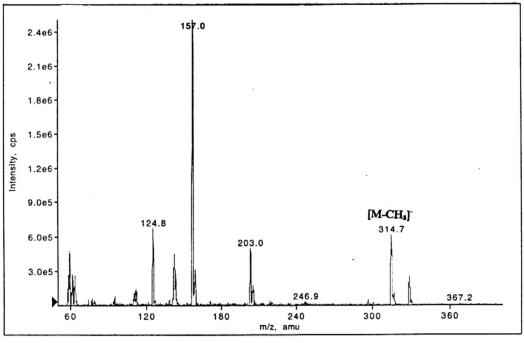

Fig.(44) -The mass spectrum of malathion exhibits a distinct peak at m/z 314.7 $[M\text{-}CH_3]^-$ or $[M\text{-}15]^-$ frament ion under NCI mode(163).

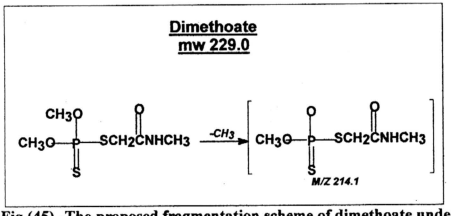

Fig.(45) -The proposed fragmentation scheme of dimethoate under NCI mode.

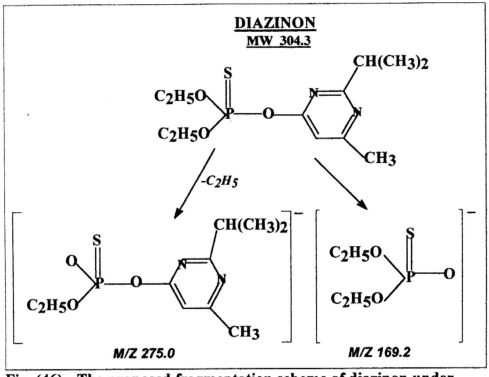

Fig. (46) - The proposed fragmentation scheme of diazinon under NCI mode (163).

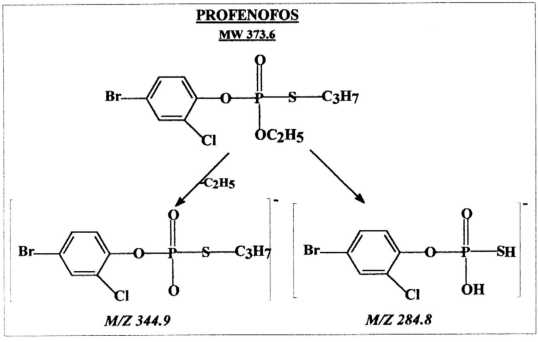

Fig. (47) - The proposed fragmentation scheme of profenofos under NCI mode (163).

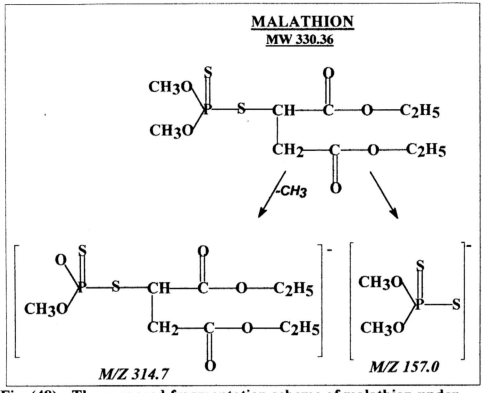

Fig. (48) - The proposed fragmentation scheme of malathion under NCI mode (163).

Chlorpyrifos which is also an interhalogen compound behaves similarly as chlorothalonil to produce the $[M-Cl+O]^-$ fragment ion of high intensity under NCI mode (163). Fig.(49,50) shows the mass spectrum and the proposed fragmentation scheme of chlorpyrifos under NCI mode.

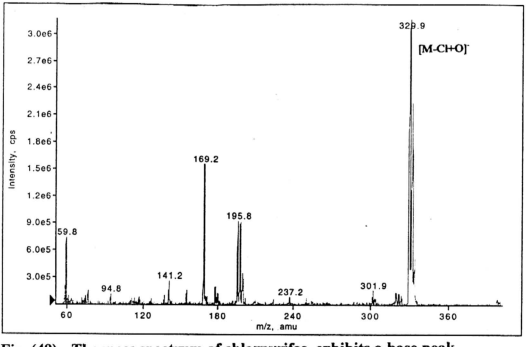

Fig. (49) - The mass spectrum of chlorpyrifos exhibits a base peak at m/z 329.9 $[M-Cl+O]^-$ or $[M-19]^-$ fragment ion under NCI mode(163).

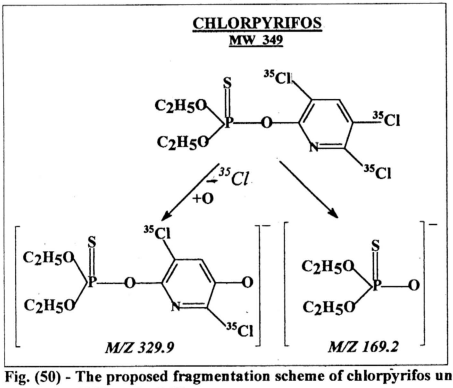

Fig. (50) - The proposed fragmentation scheme of chlorpyrifos under NCI mode (163).

Table (12) compares the sensitivities with respect to peak areas when different ions were monitored separately in the 2 chromatograms as shown in Fig. (51,52).

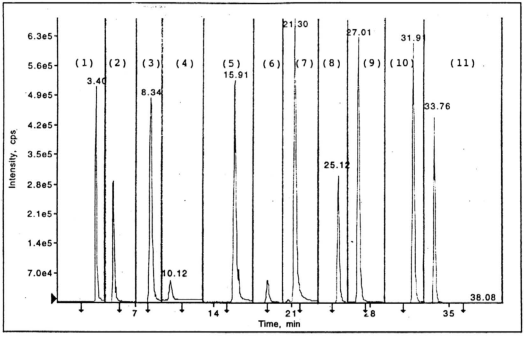

Fig.(51) - The chromatogram of the pesticides mixture when (1) methamidophos $[M+H]^+$, (2) dimethoate $[M+H]^+$, (3) carbofuran $[M+H]^+$, (4) carbaryl $[M+H]^+$, (5) diuron $[M+H]^+$, (6) methiocarb $[M+H]^+$, (7) chlorothalonil $[M-Cl+O]^-$, (8) ethyl-parathion $[M-C_2H_5]^-$, (9) diazinon $[M+H]^+$, (10) profenofos $[M+H]^+$, (11) chlorpyrifos $[M-Cl+O]^-$ were monitored under LC-API-MS(SIM).

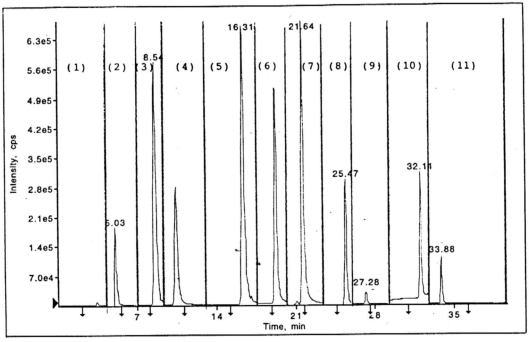

Fig. (52) - The chromatogram of pesticides mixture when (1) methamidophos $[M-H]^-$, (2) dimethoate $[M-CH_3]^-$, (3) carbofuran $[M+H-CONCH_3]^+$, (4) carbaryl $[M+H-CONCH_3]^+$, (5) diuron $[M+H]^+$, (6) methiocarb $[M+H-CONCH_3]^+$, (7) chlorothalonil $[M-Cl+O]^-$, (8) ethyl-parathion $[M-C_2H_5]^-$, (9) diazinon $[M-C_2H_5]^-$, (10)profenofos $[M-C_2H_5]^-$, (11) chlorpyrifos $[M+H]^+$ were monitored under LC-API-MS (SIM).

	Chromatogram Fig. 51			Chromatogram Fig. 52		
	Monitoring ion (m/z)	Mode of ionisation	Peak area	Monitoring ion (m/z)	Mode of ionisation	Peak area
Methamidophos	142.2$[M+H]^+$	PCI	3.86e6	140.1$[M-H]^-$	NCI	5.41e4
Dimethoate	230.2$[M+H]^+$	PCI	3.06e6	214.1$[M-CH_3]^-$	NCI	2.05e6
Carbofuran	222.3$[M+H]^+$	PCI	7.47e6	165.3$[M+H-CONCH_3]^+$	PCI	8.91e6
Carbaryl	202.4 $M+H]^+$	PCI	7.80e5	145.3 $M+H-CONCH_3]^+$	PCI	5.25e6
Diuron	233.1$[M+H]^+$	PCI	8.80e6	233.1$[M+H]^+$	PCI	9.02e6
Methiocarb	226.2$[M+H]^+$	PCI	7.86e5	169.3$[M+H-CONCH_3]^+$	PCI	7.75e6
Chlorothalonil	245.0$[M-Cl+O]^-$	NCI	1.04e7	245.0$[M-Cl+O]^-$	NCI	1.05e7
Ethyl-parathion	262.1$[M-C_2H_5]^-$	NCI	3.50e6	262.1$[M-C_2H_5]^-$	NCI	3.52e6
Diazinon	305.3 $M+H]^+$	PCI	7.99e6	275.0$[M-C_2H_5]^-$	NCI	3.80e5
Profenofos	375.0$[M+H]^+$	PCI	7.24e6	344.9$[M-C_2H_5]^-$	NCI	3.17e6
Chlorpyrifos	329.9$[M-Cl+O]^-$	NCI	4.22e6	350.1$[M+H]^+$	PCI	1.07e6

Table (12) - Comparison of the sensitivities with respect to peak areas when different ions of the same compound were monitored.

The Table (12) above clearly indicated that higher sensitivity was obtained when the fragment ion $[M+H-CONCH_3]^+$ and $[M-Cl+O]^-$ were selected for monitoring

NMCs (carbofuran, carbaryl and methiocarb) and chlorpyrifos respectively in LC-API-MS (SIM) analyses as compared to the pseudo-molecular ions $[M+H]^+$. Whereas for methamidophos, dimethoate, diazinon and profenofos, monitoring the protonated pseudo-molecular ions $[M+H]^+$ is preferred as larger peak areas are obtained compared to the negative ions. For diuron, ethyl-parathion and chlorothalonil, the same fragment ions are monitored in both the analyses.

3.1.2 Eluent Flow Rate

The method of calculating the signal-to-noise (S/N) ratio (180) is to subtract the minimum value of the background signal from the maximum background signal. This difference is then compared to the signal from the suspected presence of a chemical phenomenon. The signal is then divided by the difference of the background signal.

$$S/N = \frac{\text{signal}}{Max_{background} - Min_{background}}$$

In this study, different eluent flow rates (0.6 ml/min to 1.6 ml/min) were delivered to the heated nebuliser probe. Although the signal response remained unchanged, the use of the lower flow rates improved the base line stability, thereby increasing the signal-to-noise ratio. This is because the difference between the

maximum and minimum background signal remains more stable at lower flow rates. Fig. (53) shows the intensities of the some individual pesticide when they were run at different eluent flow rates. It clearly indicated that the optimum eluent flow rates are between 0.6 ml/min to 0.8 ml/min which gave rise to high signal-to-noise ratio of the compounds, but the elution at the flow rate of 0.8 ml/min was selected for the study as it gave good chromatographic separation of the pesticides.

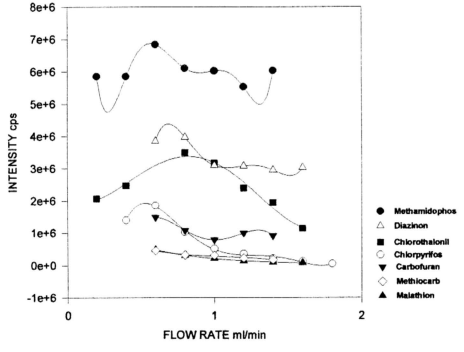

Fig. (53) - The intensities of Methamidophos, Diazinon, Chlorothalonil, Chlorpyrifos, Carbofuran, Methiocarb, and Malathion, vary with eluent flow rates.

3.1.3 Heated Nebuliser Probe Temperature

The quantity and type of sample affects the optimum heated nebuliser probe temperature. At higher flow rates, the optimum temperature increases. The heat is used to vaporise the sample and solvent sprayed into the ion source chamber. If the temperature is set too low, the vaporisation is incomplete, however setting the temperature too high induces thermal degradation of the sample. The optimum temperature is the lowest setting which ensures the complete vaporisation of the sample. A graphical presentation of the results from the optimisation of the temperatures is shown in Fig.(54).

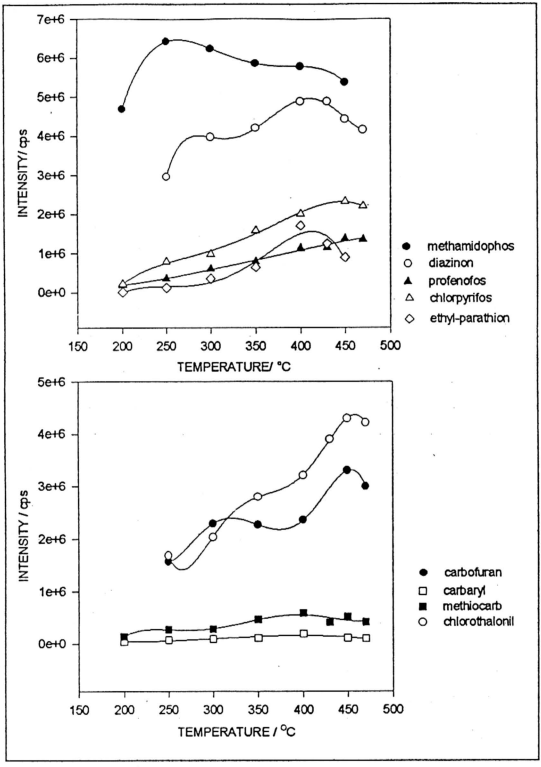

Fig. (54) - The intensity vs temperature of some pesticides

3.1.4 Orifice and Focusing ring Voltages

For the orifice and focusing ring voltages, the higher the orifice and focusing ring voltages, the greater the energy imparted to the ions entering the analysing region of the mass spectrometer. The energy helps to decluster the ions and to reduce the chemical noise in the spectrum resulting in an increase in the signal-to-noise ratio or sensitivity. By increasing the voltages beyond optimum conditions, the increased energy can induce ion fragmentation which provides the potential for generation of alternative confirmatory ions but at the expense of molecular ion sensitivity. To minimise the fragmentation and thus maximise the sensitivity for the pseudo-molecular ion and characteristic fragment ion on which quantitation was based, the orifice and focusing ring voltages should be kept low to minimise further fragmentation in the pre-analyser zone. Fig. (55) & (56) show the graphic presentations of the orifice and focusing ring voltages affecting the signal-to noise ratio.

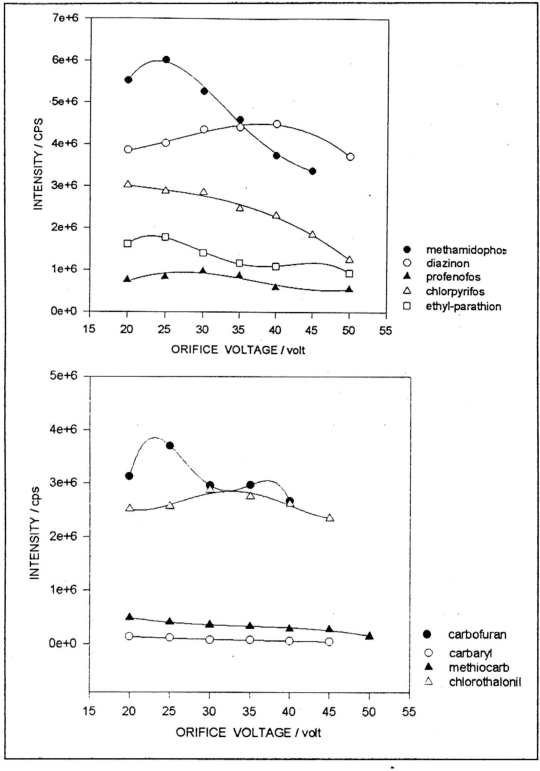

Fig. (55) - The intensity vs orifice voltage of some pesticides

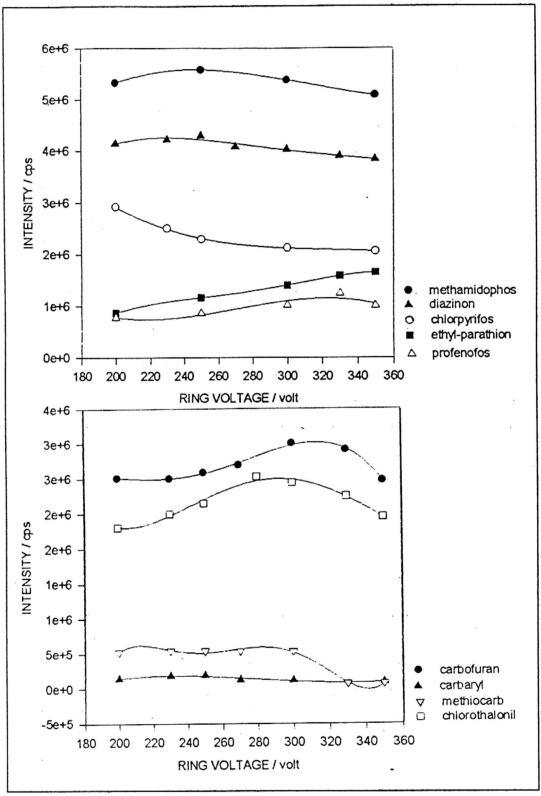

Fig. (56) - The intensity vs focusing ring voltage of some pesticides.

Table (13) shows the optimum parameters which were employed for the different pesticides- heated nebuliser probe temperature, focusing ring and orifice voltages as used in this study.

COMPOUND	HEATED NEBULISER PROBE TEMP. / °C	FOCUSING RING VOLTAGE /V	ORIFICE VOLTAGE / V
Methamidophos	250	230	20
Dimethoate	350	250	35
Carbofuran	450	300	25
Carbaryl	350	250	20
Diuron	350	300	25
Methiocarb	400	300	20
Chlorothalonil	450	-330	-35
Ethyl-parathion	400	-350	-25
Diazinon	400	230	30
Profenofos	450	330	30
Chlorpyrifos	450	200	20

Table (13): The optimum parameters - the heated nebuliser probe temperature, focusing ring voltage and the orifice voltage.

3.2 Identification and Confirmation of Pesticides

3.2.1 Collision Induced Dissociation (CID)

The selectivity of the single quadrupole MS can be considerably increased by monitoring two ions - the precursor ion derived from the intact molecule at low orifice voltage (OR=20 volts), the protonated pseudo-molecular ion $[M+H]^+$ and its major fragment ion produced at high orifice voltage (OR=60 volts), thus allowing for unambiguous pesticide identification and confirmation. Fig. (57-68) show the mass spectra of some selected pesticides scanned at OR=20 volts and OR=60 volts.

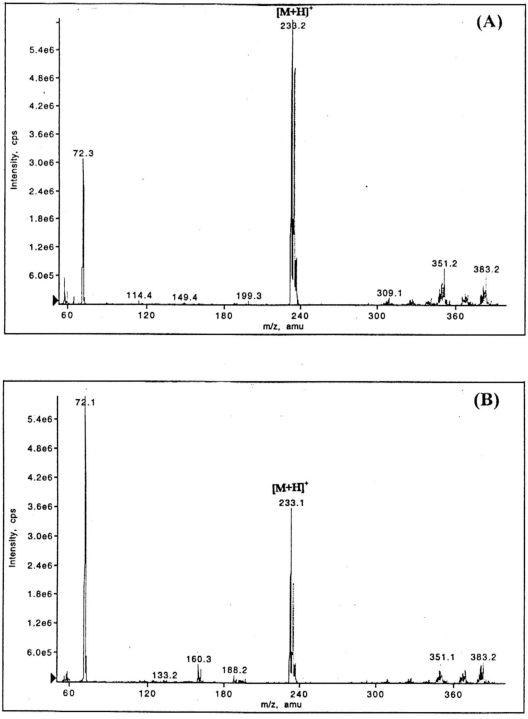

Fig. (57) - The mass spectra of diuron at low orifice V = 20 volts (A) and high orifice V = 60 volts (B) under PCI mode.

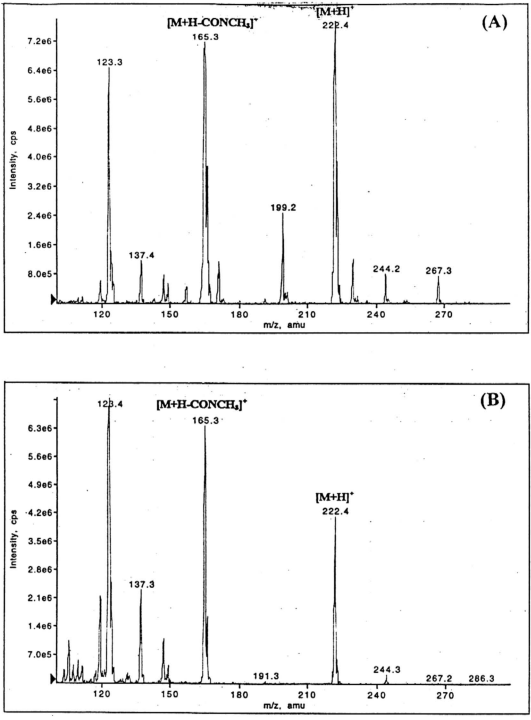

Fig. (58) - The mass spectra of carbofuran at low orifice V = 20 volts (A) and high orifice V = 60 volts (B) under PCI mode.

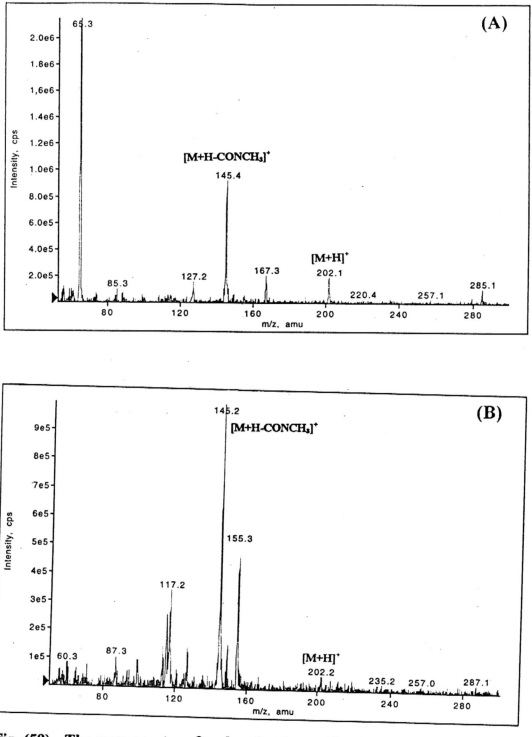

Fig. (59) - The mass spectra of carbaryl at low orifice V = 20 volts (A) and high orifice V = 60 volts (B) under PCI mode.

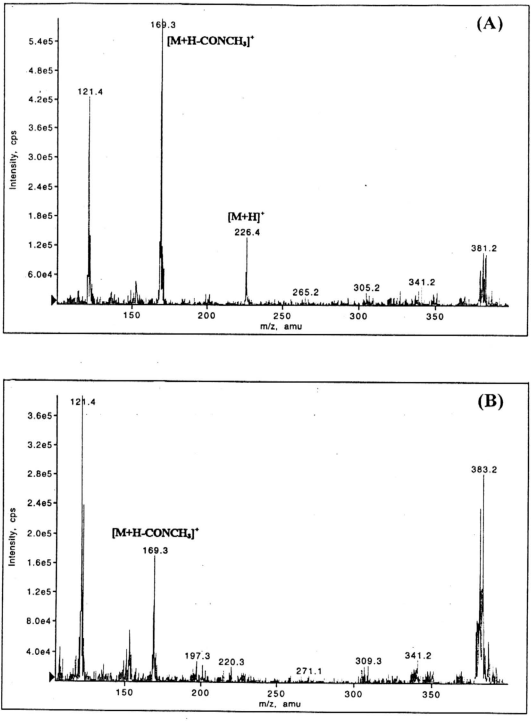

Fig. (60) - The mass spectra of methiocarb at low orifice V = 20 volts (A) and high orifice V = 60 volts (B) under PCI mode.

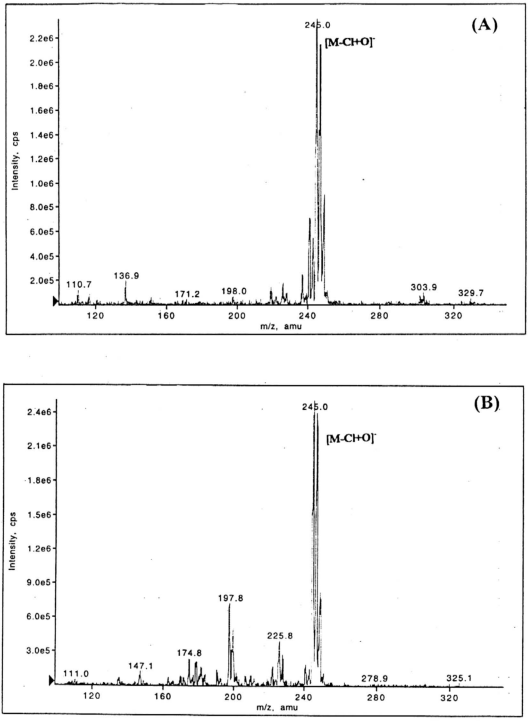

Fig. (61) - The mass spectra of chlorothalonil at low orifice V = 20 volts (A) and high orifice V = 60 volts (B) under NCI mode.

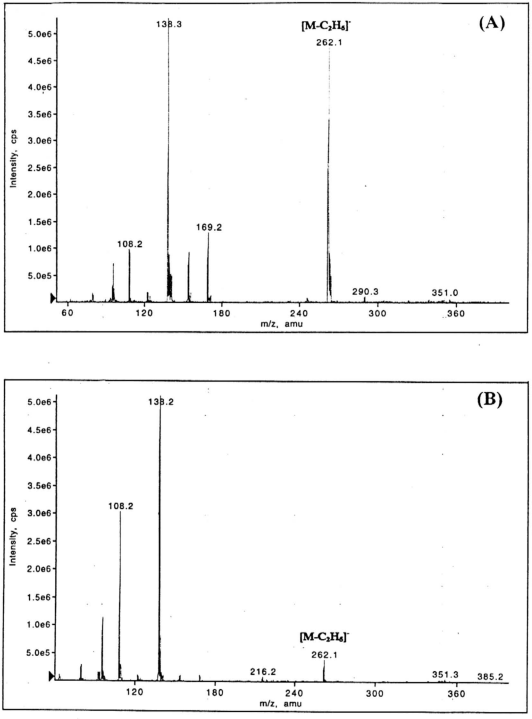

Fig. (62) - The mass spectra of ethyl-parathion at low orifice V = 20 volts (A) and high orifice V = 60 volts (B) under NCI mode.

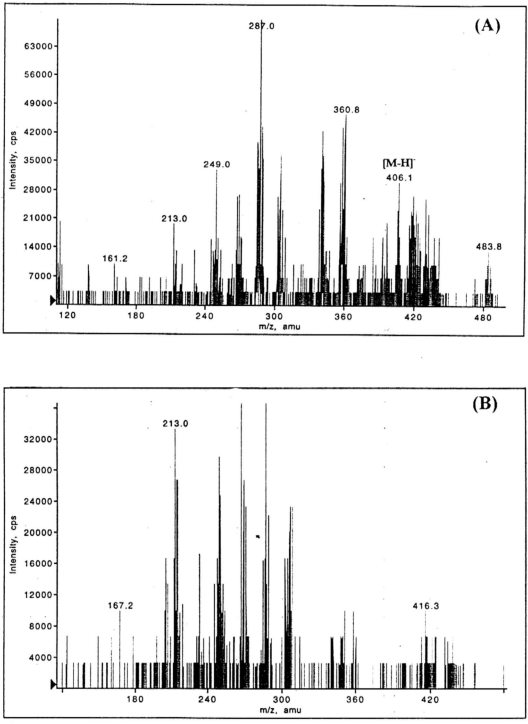

Fig. (63) - The mass spectra of endosulfon at low orifice V = 20 volts (A) and high orifice V = 60 volts (B) under NCI mode.

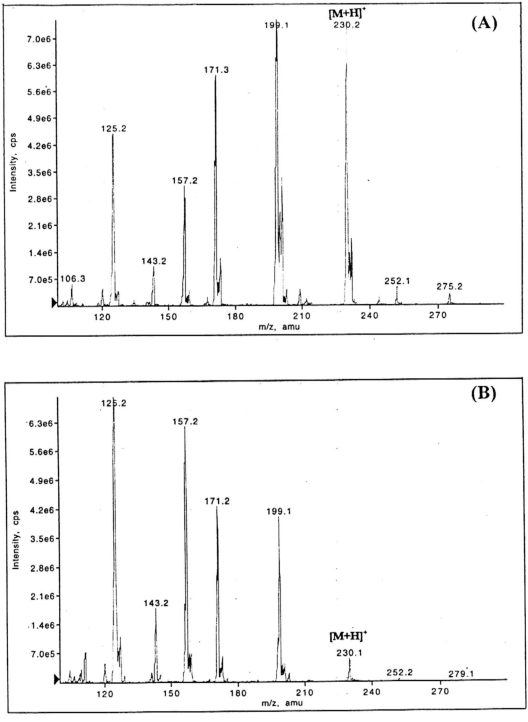

Fig. (64) - The mass spectra of dimethoate at low orifice V = 20 volts (A) and high orifice V = 60 volts (B) under PCI mode.

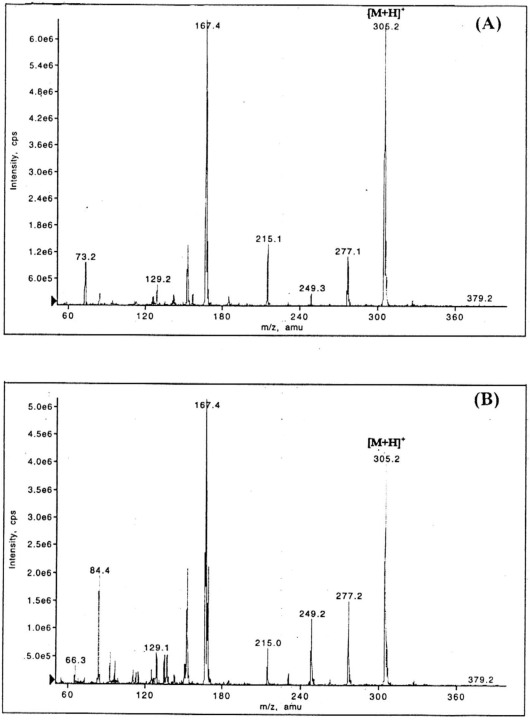

Fig. (65) - The mass spectra of diazinon at low orifice V = 20 volts (A) and high orifice V = 60 volts (B) under PCI mode

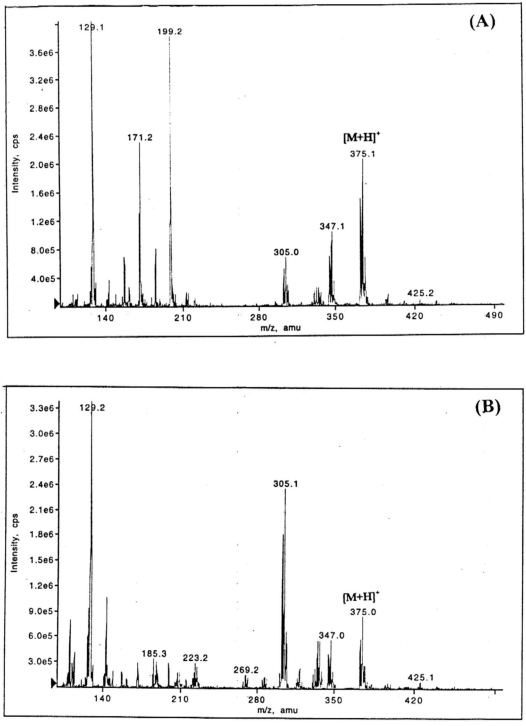

Fig. (66) - The mass spectra of profenofos at low orifice V = 20 volts (A) and high orifice V = 60 volts (B) under PCI mode

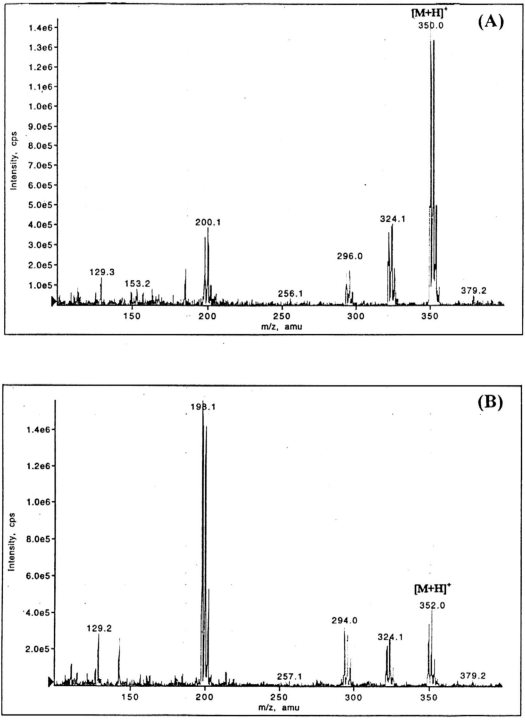

Fig. (67) - The mass spectra of chlorpyrifos at low orifice V = 20 volts (A) and high orifice V = 60 volts (B) under PCI mode

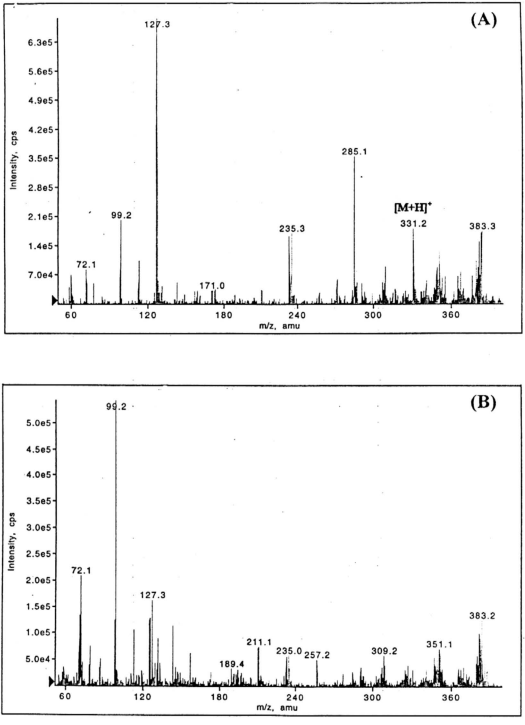

Fig. (68) - The mass spectra of malathion at low orifice V = 20 volts (A) and high orifice V = 60 volts (B) under PCI mode

3.2.2 Retention Time

In this study, emphasis on the combination of retention time data, molecular mass information from the $[M+H]^+$ or $[M-H]^-$ ion and other characteristic fragment ions provide satisfactory information for the identification of target analytes without a large risk of false positive. The % relative standard deviation (RSD) values of retention times recorded within a one week period were typically less than 2.5%. Table (14) shows the mean retention times and the %RSDs (N = 25) of the pesticides studied in the multiclass and multiresidue analysis.

Pesticide	Mean Retention Time (min)	% RSD
Methamidophos	3.38	0.45
Dimethoate	5.26	1.21
Carbofuran	9.42	1.84
Carbaryl	11.71	2.21
Diuron	17.75	1.66
Methiocarb	20.80	1.32
Chlorothalonil	23.29	1.12
Ethyl-parathion	27.27	0.75
Diazinon	28.96	0.76
Profenofos	33.82	0.62
Chlorpyrifos	35.80	0.83

Table (14) - The mean retention times and %RSD of the pesticides (%RSD=% relative standard deviation)

3.3 Clean-Up

Most environmental sample extracts will usually require a preliminary clean-up procedure before determination by LC. The extent of clean-up required is dependent on the type of sample being analysed, the detection limit required and the detection technique employed. Usually about 80% of water samples would not

require clean-up of samples or extracts. On the other hand, almost all methods for soil and plant samples require at least some clean-up. Selective detection techniques such as fluorescence or mass spectrometry may minimise the need for clean-up by ignoring the co-eluting extractives. The need for clean-up is indicated when it is not possible to separate an analyte from an interfering co-extractive on the LC column at the required level of sensitivity. Fig.(69) shows the chromatogram of a spiked control sample when no clean up steps were employed. From the chromatogram, it shows that the co-extractive material can interfere with compounds of high polarity such as methamidophos, dimethoate and the NMC pesticides. An initial attempt to use Florisil column chromatography clean up by elution with solvent mixtures of petroleum ether and diethyl ether with increasing polarity failed to produce good results because the recoveries for compounds such as methamidophos and dimethoate were low (< 50 %). Fig. (70) shows the chromatogram of a spiked sample with Florisil column clean up using 100 ml acetonitrile to elute the sample. The recoveries obtained ranged between 70% - 110% for all investigated pesticides and therefore it was selected for this study.

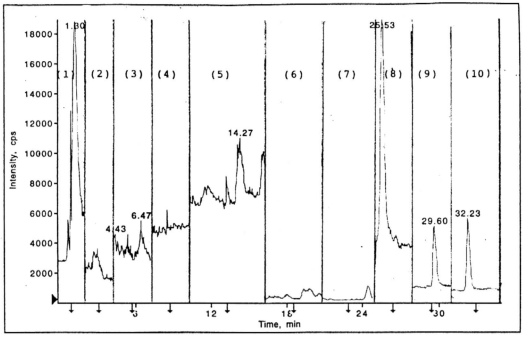

Fig. 69 - The chromatogram of a spiked control sample without clean-up. (1)methamidophos,(2)dimethoate,(3)carbofuran,(4)carbaryl,(5)methiocarb (6)chlorothalonil, (7) ethyl-parathion, (8) diazinon,(9) profenofos, (10) chlorpyrifos

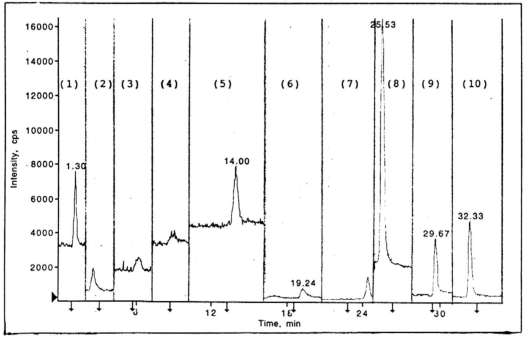

Fig. 70 – The chromatogram of a spiked control sample with Florisil column clean-up. (1) methamidophos, (2) dimethoate, (3) carbofuran, (4) carbaryl, (5) methiocarb, (6)chlorothalonil, (7) ethyl-parathion, (8) diazinon, (9) profenofos, (10) chlorpyrifos.

Development of a clean-up method is often difficult and tedious since co-extractive compounds which are similar to the analyte are those which are most difficult to remove without also removing the analyte. Therefore the aim of sample clean-up is to remove as much of the interfering co-extracted material and as little of the analyte as possible. It may also be desirable to clean-up samples in order to prolong the life-span of an HPLC column or to prevent contamination of detectors.

3.4 Detection Limits

Determination of the limits of detection (LOD) were performed on a pesticide free water spinach (*Ipomoea aquatica*) sample spiked with the mixed standard stock solution containing all 11 pesticides. The limits of detection were calculated based on S/N=3. Table (15) shows the limits of detection (LOD) of the 11 pesticides in water spinach which were obtained in the range between 1 - 3 ρg.

Pesticide	Monitoring Ion	*LOD (ρg)
Methamidophos	142.2 $[M+H]^+$	1.0
Dimethoate	230.2 $[M+H]^+$	1.0
Carbofuran	165.3 $[M+H\text{-}CONCH_3]^+$	1.5
Carbaryl	145.3 $[M+H\text{-}CONCH_3]^+$	1.5
Diuron	233.1 $[M+H]^+$	1.0
Methiocarb	169.3 $[M+H\text{-}CONCH_3]^+$	2.5
Chlorothalonil	245.0 $[M\text{-}Cl+O]^-$	1.0
Ethyl-parathion	262.1 $[M\text{-}C_2H_5]^-$	2.5
Diazinon	305.3 $[M+H]^+$	1.0
Profenofos	375.0 $[M+H]^+$	1.5
Chlorpyrifos	329.9 $[M\text{-}Cl+O]^-$	1.5

Table (15) - The monitoring ions and the limits of detection (LOD) of the pesticides in LC-API-MS analysis

Some compounds such as methamidophos and diazinon show similar LODs, even though their sensitivities are different at the optimum eluent flow rate,

temperature, orifice and focusing ring voltages as shown in Figures 53, 54, 55 and 56. This is because their noise or background levels are different for different compounds. Methamidophos shows a higher background level than diazinon as shown in Fig.(70).

3.5 Linearity of Calibration Curves

A calibration graph of each pesticide was prepared by injecting the calibration standard solutions which were prepared by appropriate dilution of the mixed standard stock solution. The calibration curves were constructed using the peak areas and concentrations of the respective pesticide in the calibration standard solutions. A representative calibration curve of methamidophos is linear for concentrations ranging from 0.1 ppm to 1.0 ppm is as shown in Fig. (71).

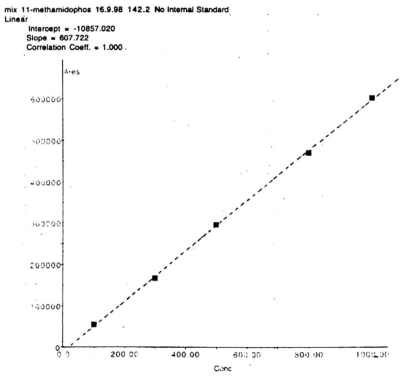

Fig. (71) - The calibration curve of methamidophos for Concentration ranging from 0.1 - 1.0 ppm

The linearity of the chromatographic determination of all the 11 pesticides was examined for 2 concentration ranges as shown in Table (16). The results of all the pesticide calibration curves are within the acceptable values for the correlation coefficient ($r^2 \geq 0.98$).

	HIGH LEVEL			LOW LEVEL		
PESTICIDES	CONC. RANGE (ppm)	CORR. COEFF. r^2	% RECOVERY	CONC. RANGE (ppm)	CORR. COEFF. r^2	RECOVERY %
Methamidophos	1.0 - 6.0	0.997	92.5	0.1 - 1.0	1.0	102.4
Dimethoate	3.0 - 18.0	0.998	100.7	0.3 - 3.0	1.0	98.9
Carbofuran	2.0 - 12.0	0.997	97.1	0.2 - 2.0	1.0	97.5
Carbaryl	3.0 - 18.0	0.997	107.9	0.3 - 3.0	1.0	100.8
Diuron	2.0 - 12.0	0.997	104.4	0.2 - 2.0	1.0	98.4
Methiocarb	5.0 - 30.0	0.999	93.4	1.5 - 5.0	0.998	94.4
Chlorothalonil	3.0 - 18.0	0.998	90.9	0.3 - 3.0	0.998	80.8
Ethyl-parathion	5.0 - 30.0	0.999	80.0	0.5 - 5.0	0.994	72.4
Diazinon	0.5 - 3.0	1.0	95.3	0.15- 0.5	1.0	91.9
Profenofos	3.0 - 18.0	0.999	92.6	0.3 - 3.0	0.996	86.4
Chlorpyrifos	5.0 - 30.0	0.999	98.7	0.5 - 5.0	0.997	81.5

Table 16 - Comparison of correlation coefficient r^2 and recoveries of pesticides at different concentration range

3.6 Recoveries of Pesticides

The recoveries of the 11 pesticides in water spinach were examined at 2 fortification levels. Duplicate samples of 30 g each of homogenised, chopped and blended vegetable were each spiked with 100 μL and 60 μL of mixed standard stock solution respectively. The spiked samples were extracted with procedures as shown in Fig.7 so as to produce the final concentrations of the pesticides as shown in Table (17). The recoveries of the pesticides ranged between 69% to 108% and % RSDs were below 10% (n = 2).

		HIGH LEVEL			LOW LEVEL		
PESTICIDES	CORR. COEFF. (r^2)	FORTIFICATION LEVEL ppb (ng/ml)	RECOVERIES %	%RSD	FORTIFICATION LEVEL ppb (ng/ml)	RECOVERIES %	%RSD
Methamidophos	1.0	500	102.4	3.05	300	107.4	4.93
Dimethoate	1.0	1500	98.9	1.35	900	97.3	4.87
Carbofuran	1.0	1000	97.5	1.74	600	94.4	4.34
Carbaryl	1.0	1500	103.2	1.07	900	107.5	7.56
Diuron	1.0	1000	98.4	4.07	600	94.1	2.66
Methiocarb	0.998	2500	94.4	0.37	1500	96.3	8.93
Chlorothalonil	0.998	1500	81.4	3.27	900	73.5	5.67
Ethyl-parathion	0.994	2500	72.4	0.39	1500	69.8	9.93
Diazinon	1.0	250	91.9	4.46	150	80.0	6.80
Profenofos	0.996	1500	86.4	5.44	900	71.8	3.44
Chlorpyrifos	0.997	2500	81.5	2.77	1500	74.3	7.04

Table 17-Correlation coefficient r^2 and recoveries of pesticides at 2 different fortification levels in water spinach "kangkong"

3.7 Precision and Accuracy

Data that are obtained as a result of analysing a chemical sample should be assessed for accuracy and precision. In this aspect, the accuracy refers to the ability of an analytical technique or analytst to portray the real quantity of an object. In this regard, the analysis portion of the method must faithfully represent the object that is analysed. Another term which is used to illustrate the accuracy is relative error. Mathematically, the accuracy is the average relative deviation of the analysis of a set of data from the mean of the population (181):

$$\text{Relative error} = \frac{\sum \frac{\overline{X} - True}{True}}{N}$$

where N is the number of determinations. The % relative error is;

$$\% \text{ Relative Error} = \frac{\sum \frac{\overline{X} - True}{True}}{N} .100$$

	% Relative Error
Methamidophos	**4.11**
Dimethoate	**2.14**
Carbofuran	**1.89**
Carbaryl	**5.34**
Diuron	**-2.78**
Methiocarb	**-4.86**
Chlorothalonil	**-6..10**
Ethyl-parathion	**-6.86**
Diazinon	**-3.90**
Profenofos	**-3.67**
Chlorpyrifos	**7.15**

Table (18) - The accuracy (% relative error) of the analysis when N = 4

The precision requires several components including repeatability and reproducibility to describe its behaviour. Repeatability as defined by the American Society for Testing and Materials (ASTM) (182), is the ability of an analytical method when repeated several times in a single day by a single analyst to give the same answer. Reproducibility is defined as the ability of an analytical method to give the same answer on different days by different analysts and possibly even in different laboratories.

Mathematically the precision may be described as the relative standard deviation from the mean of all analyses that are performed on a single sample:

$$\text{Relative standard deviation} = \frac{\sigma_{n-1}}{\overline{X}}$$

In this study, the repeatability of this analytical method was calculated based on a spiked sample prepared in duplicates on the same day, whereas the reproducibility was based on the mean repeatability values for 4 different occasions within 2 weeks period. The results are as shown in Table (19).

	Repeatability (n=2)		Reproducibility (n=4)	
	Recovery	% RSD	Recovery	% RSD
Methamidophos	92.46	2.99	91.73	4.55
Dimethoate	101.27	0.45	88.16	12.38
Carbofuran	97.42	3.15	86.85	14.18
Carbaryl	107.91	4.43	94.28	12.53
Diuron	104.41	1.38	96.93	6.29
Methiocarb	92.37	3.65	88.73	8.01
Chlorothalonil	90.95	4.28	83.44	6.04
Ethyl-parathion	71.10	3.80	69.53	13.87
Diazinon	95.27	5.13	94.38	5.44
Profenofos	92.62	2.50	90.95	6.42
Chlorpyrifos	98.67	2.81	91.90	3.37

Table (19) - The repeatability and reproducibility of multiclass and multiresidue analysis using LC-API-MS

3.8 Application on Real samples

The potential of this multiclass and multiresidue analytical method was demonstrated on 3 types of leafy vegetables; water spinach (*Ipomoea aquatica*),

choysam(Chinese Mustard - *Brassica chinensis var. para chinensis*) and kailan (Chinese Kale - *Brassica alboglabra*) which were obtained from the local market. Each analysis includes 2 recovery samples and one control sample. All pesticides showed recoveries of between 80% to 110% except ethyl-parathion (69.5% - 80.1%), which was probably due to a lower sensitivity in the chromatographic determination. Table (20) shows the correlation coefficients r^2 and the recoveries of pesticides in 3 different type of vegetables. Table (21) shows the pesticide levels detected in the vegetables. Table (22) shows the MRLs given by Food Act 1983 (184) and Codex Alimetarius (185).

	WATER SPINACH		CHOYSAM		KAILAN	
PESTICIDES	CORR. COEFF. r^2	RECOVERIES %	CORR. COEFF. r^2	RECOVERIES %	CORR. COEFF. r^2	RECOVERIES %
Methamidophos	1.000	102.4	0.999	98.3	0.997	92.5
Dimethoate	1.000	98.9	0.999	97.8	0.998	100.7
Carbofuran	1.000	97.5	0.989	100.0	0.997	97.1
Carbaryl	1.000	103.2	0.985	96.4	0.997	107.9
Diuron	1.000	98.4	0.998	95.3	0.997	104.4
Methiocarb	0.998	94.4	0.994	109.1	0.999	92.4
Chlorothalonil	0.998	81.4	0.998	95.1	0.998	90.9
Ethyl-parathion	0.994	72.4	0.994	80.1	0.998	69.5
Diazinon	1.000	91.9	0.998	93.5	1.000	95.3
Profenofos	0.996	86.4	0.997	98.3	0.999	92.6
Chlorpyrifos	0.997	81.5	0.998	99.5	0.999	98.7

Table 20- The correlation coefficient r^2 and recoveries of pesticides in 3 different types of vegetables

	PESTICIDE LEVEL ng/g (ppb)		
PESTICIDE	**WATER SPINACH**	**CHOYSAM**	**KAI LAN**
Methamidophos	**nd**	**nd**	**nd**
Dimethoate	**0.398**	**nd**	**nd**
Carbofuran	**0.702**	**0.571**	**nd**
Carbaryl	**nd**	**nd**	**nd**
Diuron	**0.205**	**0.862**	**nd**
Methiocarb	**nd**	**nd**	**nd**
Chlorothalonil	**nd**	**nd**	**nd**
Ethyl-parathion	**nd**	**nd**	**nd**
Diazinon	**nd**	**0.410**	**nd**
Profenofos	**nd**	**nd**	**nd**
Chlorpyrifos	**nd**	**1.535**	**nd**

Table (21) - The pesticide levels in the vegetables. (nd = not detected)

	MAXIMUM RESIDUE LEVELS (MRL)	
PESTICIDES	FOOD ACT 1983 mg/kg (ppm)	CODEX ALIMENTARIUS mg/kg (ppm)
Methamidophos	1.0	1.0
Dimethoate	2.0	1.0
Carbofuran	0.5	0.5
Carbaryl	10.0	10.0
Diuron	0.2	NA
Methiocarb	0.2	0.2
Chlorothalonil	5.0	5.0
Ethyl-parathion	0.7	0.7
Diazinon	0.7	0.5
Profenofos	0.5	NA
Chlorpyrifos	1.0	1.0

Table. 22- Maximum residue levels (MRLs) given by Food Act 1983 (184) And Codex Alimentarius (185). (NA = not available)

3.9 Measurement for some selected pesticide formulations

Using the FIA-API-MS system, calibration graphs of each pesticide were prepared by injecting the 4 standard solutions (1 ppm, 3 ppm, 5 ppm, 8 ppm) which were prepared by appropriate dilution of the respective standard stock solution. Pesticides were detected by using the selected ion monitoring (SIM) mode on the most abundant ions $[M+H]^+$ or characteristic fragment ions of the active ingredient compounds. Table (23) shows the analysis results of the pesticide formulations.

No	Source	Type of formulation	Active Ingredient	Corr. coeff, r^2	Labelled Value	Experimental value
1	DOA	Carbaryl	carbaryl	0.990	5%	7.21%
2	DOA	Carbofuran	carbofuran	1.0	3%	3.81%
3	DOA	Methiocarb	methiocarb	0.989	50%	47.05%
4	DOA	Chlorothalonil	chlorothalonil	0.997	40%	42.3%
5	DOA	Endosulfan	endosulfan	0.983	33%	37.8%
6	HEXTAR	Endosulfan	endosulfan	0.983	33%	28.98%
7	FIELD	Endosulfan	endosulfan	0.983	32%	33.71%
8	DOA	Diazinon	diazinon	0.999	53%	56.7%
9	DOA	Malathion	malathion	0.991	80%	85.6%
10	DOA	Dursban	chlorpyrifos	0.989	21.2%	20.06%
11	HEXTAR	Hextar38.7%	chlorpyrifos	0.989	38.7%	32.34%
12	HEXTAR	Hextar21.2%	chlorpyrifos	0.989	21.2%	22.31%
13	FIELD	Dursban	chlorpyrifos	0.989	20%	23.67%
14	FIELD	Zesban 45%	chlorpyrifos	0.989	45%	35.08%
15	FIELD	Nurelle	chlorpyrifos	0.989	45.9%	42.79%
16	DOA	Methamidophos	methamidophos	0.999	50%	37.47%
17	HEXTAR	Hextar50%	methamidophos	0.999	50%	57.2%
18	FIELD	Multiphos	methamidophos	0.999	50%	38.33%

Table (23). Results of pesticide formulations using FIA-API-MS